Volume 1 | Number 1 | Jan 2013 | Pages 1–100

Dalton Transactions

An international journal of inorganic chemistry
www.rsc.org/dalton

ROYAL SOCIETY OF CHEMISTRY

ROYAL SOCIETY OF CHEMISTRY

www.rsc.org/dalton

Dalton Transactions

COMMUNICATION

Decoration of the layered manganese oxide birnessite by Mn(II/III) gives a new water oxidation catalyst with fifty-fold turnover number enhancement.

Ian G. McKendry, Sandeep K. Kondaveeti, Samantha L. Shumlas, Daniel R. Strongin,* and Michael J. Zdilla*

The role of manganese average oxidation state (AOS) on water oxidation catalysis by birnessite was investigated. Low AOS samples were most active, generating O_2 immediately. Samples with a relatively high AOS showed an initial induction period and decreased turnover. Mn(II- and III)-enriched samples gave a 10-50 fold enhancement in turnover number.

The production of solar hydrogen is a grand challenge of green energy science due to the low cost and renewability of two of the most abundant resources on the planet: water and sunlight.[1] One of the remaining hurdles is the development of an effective catalyst for water oxidation. In photosynthetic plants, photosystem II carries out this chemistry, and comprises a water-accessible $CaMn_4O_5$ cluster entitled the oxygen evolving complex (OEC) in the enzyme active site.[2] Due to their fragility, however, enzymes are generally not viable for industrial scale processes. Instead, such catalytic systems must be robust, cheap, and made from environmentally friendly, earth abundant elements. Metal oxides are a promising class of catalytic materials that satisfy these criteria.

One particular metal oxide system of interest is birnessite, MnO_2, a layered, mixed Mn(III/IV) manganese oxide with interstitial water molecules and Lewis acid cations (e.g., K, Na^+, and/or Ca^{2+}(Figure 1). The presence of Lewis acidic interlayer cations and accessibility of water has made this material of particular interest due to analogy to the OEC. Several recent reports on this material are particularly noteworthy. First, Kurz and coworkers showed that birnessites with varied intercalated Lewis acid cations showed different activities, with Ca^{2+} and Sr^{2+} being most effective (analogous to the OEC).[3] However, to our knowledge there have been no

studies assessing the role of the oxidation state of Mn on chemical water oxidation by birnessite. In fact, the more effective Sr- and Ca-containing catalysts reported previously also tended to be associated with birnessite with lower average oxidation states of Mn.[4] Second, Takashima et al. demonstrated that Mn^{3+} has a role in lowering the overpotential for electrochemical water oxidation on birnessite.[5] Third, Dau and Dreiss demonstrated that mixed oxidation state MnO nanoparticles are effective water oxidation catalysts.[6] Finally, Dismukes and coworkers demonstrated that the bulk birnessite phase is an inefficient catalyst for water oxidation by ruthenium tris(bipyridine) due to the paucity of Mn^{3+} sites.[7] In this report, we demonstrate by using synthetic birnessite with varying $Mn^{2+}/Mn^{3+}/Mn^{4+}$ ratios that average oxidation state (AOS) plays an important role in chemical water oxidation by birnessite catalysts. We also experimentally demonstrate a 50-fold turnover number (TON) enhancement for water oxidation by enriching synthetic birnessite with Mn^{2+} and Mn^{3+}. This decoration produces a catalyst with a water oxidation activity higher than what has been previously reported for any birnessite.
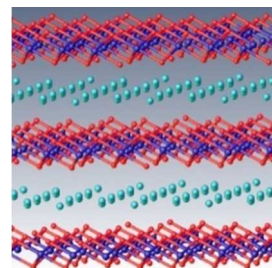
Figure 1. Structure of idealized crystalline Potassium Birnessite[8] showing Mn-O layers with interstitial K^+ ions.

Synthetic birnessite samples were prepared by reaction of permanganate with chloride ion as a reductant in boiling water.[9] By varying the ratio of permanganate to chloride, samples were prepared having varying relative proportions of Mn(IV), Mn(III), and Mn(II). The relative proportion associated with a particular birnessite sample throughout this contribution is given as the average oxidation state (AOS). The synthetic birnessite materials were analyzed for AOS using X-ray photoelectron spectroscopy (XPS). We point out that XPS is inherently surface sensitive and hence, provided the AOS of those Mn atoms in the near surface region. The materials consisted predominantly of Mn(IV) and Mn(III) based upon XPS,[10] with the surface AOS ranging from 3.45 to 3.78. This range of AOS for birnessite is consistent with prior studies that have used a similar synthetic protocol.[11] The identity of the materials was confirmed with X-ray diffraction (XRD), and the morphology of all materials determined by scanning electron microscopy (SEM) was similar (Figure 2). Brunauer-Emmett-Teller (BET) measurements indicated that the material was mesoporous with pore sizes of 2-50 nm.
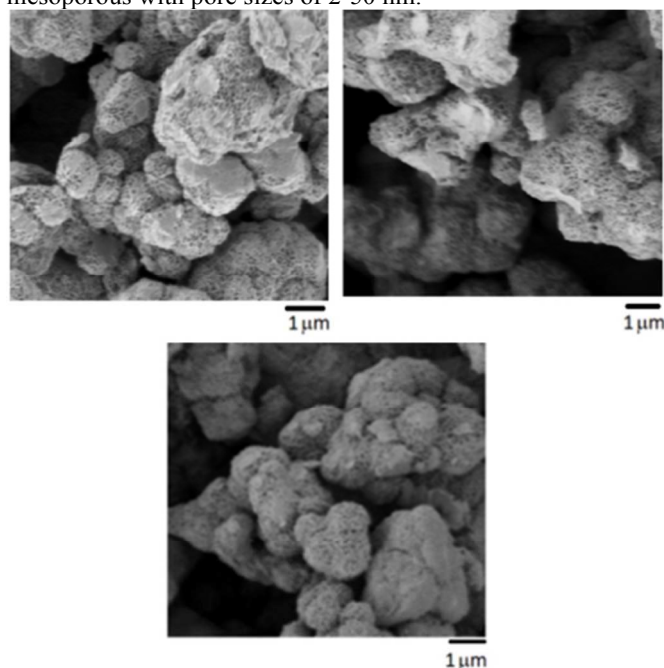
Figure 2. SEM images of three birnessite samples. Left: Pre-catalysis (B6), right: post catalysis (B6-PC), bottom: Mn(III) enriched (B6*).

Synthetic birnessite samples were tested for water oxidation catalysis by reaction with ceric ion in an unbuffered acidic (pH=2 due to the introduction of ammonium ion) aqueous solution. O_2 formation was monitored using a dissolved oxygen probe. The results of the oxygen evolution experiments are presented in Figures 3 and 4. The pH dropped to ~1 by the end of reaction due to the production of additional H^+ ions from water oxidation. O_2 evolution is normalized by catalyst loading (both surface area and bulk) for side-by-side comparison. In these plots, two distinct regions are worthy of note. First, in Figure 3A, there is the linear steady-state region, which can be observed after the first 30 seconds of reaction. In this time period, the surface AOS is similar in all samples (3.7). Noting that there is some scatter in individual runs, steady state rates are reasonably similar and total yield, TOF, and TON are

similar or slightly higher for the initial Mn(II)- and Mn(III)-rich catalysts (B1-B4) than for Mn(IV) rich catalysts B5 and B6[i] Low initial Mn(IV):Mn(III):Mn(II) ratios of ~55:40:5 gave a TON of 340 ± 180 mmol O_2/mol surface Mn, and high initial Mn(IV):Mn(III):Mn(II) ratios of ~ 80:20:0 gave a TON of 150 ± 40 mmol O_2/mol surface Mn.

The second, and more significant area of interest is the first 5 seconds of reaction (Figure 3B) in which an induction period can be observed in the Mn(IV)-rich samples, but not in the Mn(II/III)-rich samples. While there is some noise in the data during the induction period due to dilution effects from the injection, this induction is reproducible over multiple trials, and is statistically significant (see error bars from duplicate trials, Figure S8). The immediate generation of O_2 in the low AOS samples overwhelms the injection/dilution noise, and suggests low oxidation state manganese is important for water oxidation turnover. For the Mn(IV)-rich samples, initial turnover is slow, until the catalyst is activated by an unknown mechanism to begin producing O_2. After reaching the steady state (plateau) region, catalyst samples were recycled by filtration and washing with water and analyzed by XPS. All samples show a higher surface AOS after use (see Table S1). When reintroduced to a catalytic reaction, the recycled catalysts all show an induction period and lower overall performance consistent with high AOS samples. It is interesting to note that this induction period can be seen in the first ten seconds of previous reports for the higher oxidation state birnessites as well.[4]

To further test the hypothesis that low oxidation state manganese is key to catalysis of water oxidation by Ce^{4+}, we prepared samples enriched with Mn (II) and Mn(III) by addition of aqueous Mn^{2+}. The Mn(III) forms via comproportionation of the Mn(IV) in the birnessite samples with Mn(II) ions in aqueous solution:

$$[Mn^{IV}O_2]_n (s) + Mn^{II} (aq) \rightarrow [Mn^{III}O_2]_n (s) + Mn^{III} (aq)$$
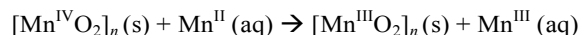
XPS confirmed enrichment by Mn(II) and Mn(III) (Table 1), and SEM and XRD showed no change in particle morphology (Figures 2, S2 and S3). TEM[†] and BET analysis indicated that an additional phase of nanoparticulate Mn(III) oxide was also formed via the comproportionation. The catalytic activity of the sample improved upon removal of this secondary phase by filtration, suggesting this phase is not the active catalyst, and may in fact inhibit catalysis. The AOS of the resulting comproportionated birnessite as measured by XPS was 3.49, compared to its initial value of 3.77.

As expected, the high-AOS catalyst lost its induction period behavior after low-AOS enrichment. To our surprise however, these catalysts exhibited up to a 50-fold enhancement in O_2 yield over the unenriched catalysts (Fig 4). This effect is illustrated by comproportionated B5* sample, where the AOS has been reduced from 3.77 to 3.49. The resulting catalyst has a TON of 5790 mmol O_2/ mol surface Mn. This comproportionated sample (AOS of 3.49) is much more active than synthetic birnessite samples with similar AOS values (e.g., B1-B4). Hence, the improvement in catalytic activity of the comproportionated B5* catalyst over other Mn(II/III)-rich catalysts (B1-B4) suggests that the bulk birnessite phase is not the active catalyst, but rather, that the enrichment by low-oxidation state Mn results in a new catalyst where birnessite is decorated by highly active catalytic surface or interlayer sites. Unlike the unmodified birnessite samples, which show high steady-state AOS of about 3.7, the Mn(II) doped birnessite

(B5*) retained a lower AOS (3.4) during catalysis (See Table S1). Combined with the excellent catalysis by these materials, the results indicate doping with aqueous Mn(II) results in catalytically active, low oxidation state defect sites that retain the low oxidation state more effectively than the bulk Mn sites. An analysis of post-reaction samples with XPS and ICP-OES shows that the dead catalyst has slightly lower AOS for the comproportionated sample (B5) of 3.44 as compared with unmodified birnessite (B3) post catalysis, which has an AOS of 3.57. Additionally, Ce^{3+}/Ce^{4+} has replaced K^+ in the interlayers after catalysis in all samples based upon XPS and ICP-OES.
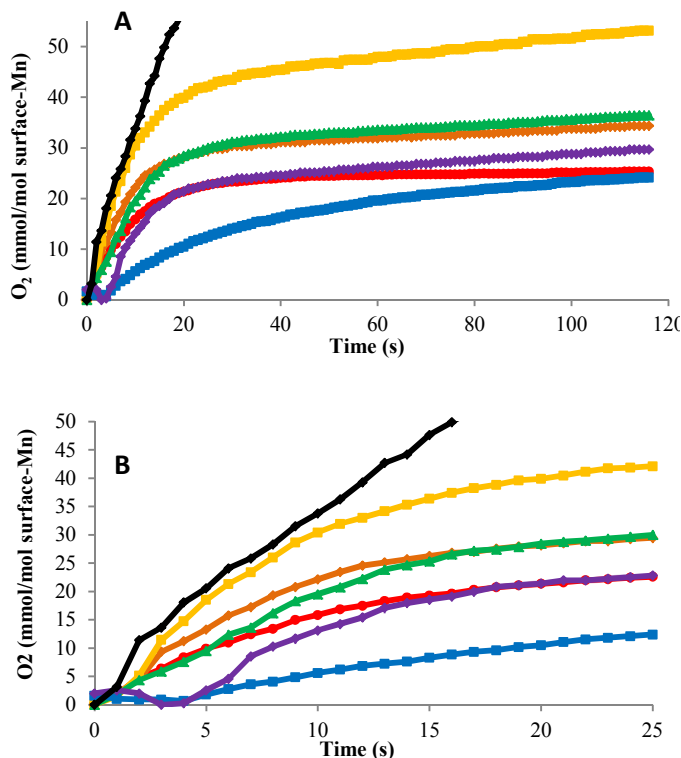
Figure 3. O_2 evolution measured by dissolved oxygen probe. Concentrations of O_2 for each sample are normalized by surface Mn. Initial AOS(sample name): ●: 3.45(B1) ◆: 3.46 (B2) ■: 3.50(B3) ▲: 3.51(B4) ■: 3.77(B5) ◆: 3.78(B6) ◆: 3.49 (B5*). A: Full time course. AOS in steady state region (> 30 s) is ca. 3.7, except for B5*, which is ca. 3.4. B: view of the early stages of reaction showing ca. 5 s induction periods for higher initial-AOS samples.

Table 1. Turnover number and turnover frequency (TOF) values for birnessite catalysts as a function of AOS. Entries are normalized by mmol surface Mn [mmol bulk Mn].

Sample	TON[a]	TOF[b]	AOS
B1	145[8.6]	2.2[0.13]	3.45
B2	535[9.6]	3.1[0.15]	3.46
B3	225[9]	4.6[0.20]	3.50
B4	454[10]	1.9[0.12]	3.51
B5	178[9.8]	0.98[0.05]	3.77
B6	115[6]	2.7[0.09]	3.78
B5*	5800[640]	4.7[0.5]	3.49

[a] TON units: mmol O_2/mol surface Mn [mmol O_2/mol Mn]
[b] TOF units: mmol O_2/mol surface Mn·s [mmol O_2/mol Mn·s]
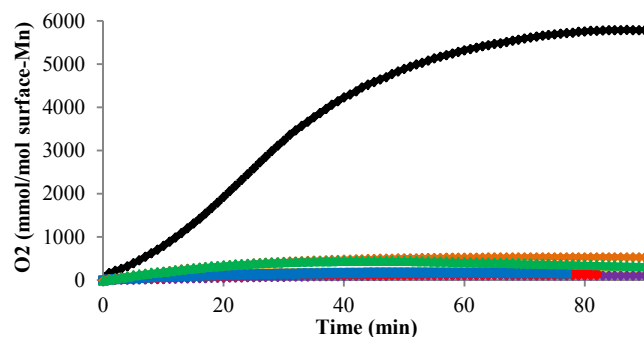
Figure 4. O_2 evolution curve measured by dissolved oxygen probe. Concentrations of O_2 for each sample are normalized by the total catalyst surface area. Initial AOS(sample name)- –: 3.45(B1) –: 3.46 (B2) –: 3.50(B3) –: 3.51(B4) –: 3.77(B5) –: 3.78(B6) –: 3.49 (B5*).

The turnover frequencies (TOF) associated with our samples B1-B6 are consistent with the majority of the prior studies of water oxidation on birnessite. Kurz and coworkers have shown that Ca-birnessite exhibits a higher activity then the K-birnessites (B1-B6) used in this and prior studies.[12] The best Ca-birnessite exhibits a water oxidation TOF of 3.96 mmol O_2/mol surface Mn*s (8.00×10^{-5} mmol O_2/m^{-2}*s), and was linked to the OEC by compositional analogy.[3] In addition to the 50-fold TON enhancement, our Mn(III) decorated sample shows a higher TOF of 4.28 mmol O_2/mol surface Mn*s (9.64×10^{-5} mmol O_2/ m^{-2}*s). Thus, the enhancement of water oxidation on K-birnessite can be accomplished by manipulating the relative proportions of manganese oxidation states in addition to the use of interlayer cations such as Ca, or via the use of high-temperature tempering.[3]

Conclusions

Our results demonstrate that low-oxidation state Mn is a key to water oxidation catalysis on this material, and is consistent with previous findings that Mn(III) is important for water oxidation catalysis in general.[3-7, 13] While Mn(II) content is also higher in the low AOS samples, previous work suggests that the Mn(II) state is inactive,[6] and we therefore tentatively ascribe the catalytic activity to Mn(III)-based active sites, though the involvement of Mn(II) cannot be strictly ruled out. Our results show that the judicious modification of birnessite with low oxidation state defect sites improves the number of turnovers achievable with this material. These results will help guide future efforts in the development of robust, affordable water oxidation catalysts.

Notes and references

[a] Department of Chemistry, Temple University, 1901 N. 13th St., Philadelphia, PA 19122.

[i] (due to the time constant of the oxygen probe (~13s), the calculated TOFs represent a lower-bound measurement of catalytic rate. The catalysts may actually be faster than reported here).

* dstrongi@temple.edu

* mzdilla@temple.edu

1. M. G. Walter, E. L. Warren, J. R. McKone, S. W. Boettcher, Q. Mi, E. A. Santori and N. S. Lewis, *Chem. Rev.*, 2010, 110, 6446-6473.

2. R. Pokhrel and G. W. Brudvig, *Phys. Chem. Chem. Phys.*, 2014, 16, 11812-11821.

3. C. E. Frey, M. Wiechen and P. Kurz, *Dalton Trans.*, 2014, 43, 4370-4379.

4. M. Wiechen, I. Zaharieva, H. Dau and P. Kurz, *Chem. Sci.*, 2012, 3, 2330-2339.

5. T. Takashima, K. Hashimoto and R. Nakamura, *J. Am. Chem. Soc.*, 2012, 134, 18153-18156.

6. A. Indra, P. W. Menezes, I. Zaharieva, E. Baktash, J. Pfrommer, M. Schwarze, H. Dau and M. Driess, *Angew. Chem. Int. Ed.*, 2013, 52, 13206-13210.

7. D. M. Robinson, Y. B. Go, M. Mui, G. Gardner, Z. Zhang, D. Mastrogiovanni, E. Garfunkel, J. Li, M. Greenblatt and G. C. Dismukes, *J. Am. Chem. Soc.*, 2013, 135, 3494-3501.

8. J. E. Post and D. R. Veblen, *American Mineralogist*, 1990, 75, 477-489.

9. R. M. McKenzie, *Mineral. Mag.* , 1971, 38, 493-502.

10. H. W. Nesbitt, G. W. Canning and G. M. Bancroft, *Geochimica et Cosmochimica Acta*, 1998, 62, 2097-2110.

11. W. Zhao, H. Cui, F. Liu, W. Tan and X. Feng, *Clays and Clay Minerals*, 2009, 57, 513-520.

12. C. E. Frey, M. Wiechen and P. Kurz, *Dalton Trans.,* 2014, 43, 4370-4379.

13. N. Birkner, S. Nayeri, B. Pashaei, M. M. Najafpour, W. H. Casey and A. Navrotsky, *Proc. Natl. Acad. Sci. USA*, 2013, 110, 8801-8806, S8801/8801-S8801/8807.

Dalton Transactions Accepted Manuscript

$$4\ Ce^{4+} + 2\ H_2O \qquad\qquad 4\ Ce^{3+} + 4\ H^+ + O_2$$